Two-Phase Mechanism of Silver Nanoparticles Against *Escherichia coli* O157:H7 Cells

กลไกการทำงานแบบสองระยะของอนุภาคเงินนาโนต่อการทำลายเชื้อ *Escherichia coli* O157:H7

Punpimon Dechsiri (พรรณพิมล เดชศิริ)* Dr.Rina Patramanon (ดร.รินา ภัทรมานนท์)**

ABSTRACT

Silver nanoparticles (AgNPs) have broad spectrum of antimicrobial activities against bacteria, fungi and virus. Nevertheless, the mechanism of AgNPs against bacterial cell is still not clear. In this study, the mechanism of AgNPs on *Escherichia coli* O157:H7 cells were determined and atomic force microscope (AFM) was employed to visualize membrane damage of *E. coli* O157:H7 due to AgNPs. The results show that AgNPs inhibited the growth of *E. coli* O157:H7 at 16 µg/ml. AgNPs display two-phase mechanism: First (fast action): AgNPs showed rapid action resulting in 88% bacterial killing within 5 min and bactericidal activity within 1 hour, causing the direct damage cells membrane as observed by AFM. The AFM images of bacterial cell treated with AgNPs for 1 hour were analyzed. The nanoscale image showed vesicles appeared on the bacterial surface membrane, leading to morphological alteration. Leakage of cytosol was also found. Second (slow action): the reactive oxygen species (ROS) were produced 2-5 hours after the AgNPs treatment. This indicated the independent event between killing and ROS production, leading to our conclusion that in the mechanism of AgNPs, ROS produced is not related with cells death.

บทคัดย่อ

งานวิจัยก่อนหน้านี้พบว่าอนุภาคเงินนาโนมีฤทธิ์ในการยับยั้งเชื้อก่อโรคได้อย่างกว้างขวาง เช่น แบคทีเรีย ฟังไจ และไวรัส แต่ถึงอย่างไรก็ตามกลไกการทำลายเชื้อแบคทีเรียของอนุภาคเงินยังคงไม่ชัดเจน ดังนั้นในงานวิจัยนี้ผู้วิจัยจึงได้ทำการศึกษากลไกการทำงานของอนุภาคเงินนาโนต่อเซลล์แบคทีเรีย *E. coli* สายพันธุ์ O157:H7 และสังเกตการเปลี่ยนแปลงลักษณะพื้นผิวด้านนอกของเซลล์แบคทีเรียในระดับนาโนด้วยเครื่องจุลทรรศน์แรงอะตอม จากผลการทดลองพบว่า อนุภาคเงินนาโนสามารถยับยั้งเชื้อแบคทีเรียได้ที่ความเข้มข้น 16 ไมโครกรัมต่อมิลลิลิตรและอนุภาคเงินนาโนมีกลไกการทำงานแบ่งออกเป็น 2 ระยะ คือ ระยะที่ 1 อนุภาคเงินสามารถยับยั้งแบคทีเรียอย่างรวดเร็วภายใน 5 นาทีและแบคทีเรียตายทั้งหมดภายใน 1 ชั่วโมง โดยภาพจากกล้องจุลทรรศน์แรงอะตอมที่สามารถตรวจสอบลักษณะพื้นผิวเซลล์ในระดับนาโน พบว่าอนุภาคเงินจะเข้าทำลายบริเวณเยื่อหุ้มเซลล์โดยตรง ทำให้เซลล์เกิดความเสียหายและตายในที่สุด ในขณะที่ระยะที่ 2 เซลล์แบคทีเรียจะมีการสร้าง ROS ขึ้นมาในเวลา 2-5 ชั่วโมงหลังจากบ่มด้วยอนุภาคเงินนาโน ดังนั้นจะเห็นได้ว่าการสร้าง ROS ไม่เกี่ยวข้องกับการตายของเซลล์แบคทีเรีย

Keywords: Silver nanoparticle (AgNPs), Mechanism, Atomic force microscope (AFM)

คำสำคัญ: อนุภาคเงินนาโน กลไกการทำงาน กล้องจุลทรรศน์แรงอะตอม

* *Student, Master of Science Program in Biochemistry, Department of Biochemistry, Faculty of Science, Khon Kaen University*

** *Associate Professor, Department of Biochemistry, Faculty of Science, Khon Kaen University*

Introduction

In the present, bacteria have been increasing in resistance against antibiotics and antimicrobial peptides (Appelbaum, 1992). Silver nanoparticles (AgNPs) are new alternative for therapeutic strategy because they have strong inhibition and bactericidal effect against bacteria, fungi and virus (Li et al., 2010). However, the antimicrobial mechanism of silver nanoparticles is still not clear. Therefore, understanding the antimicrobial mechanism is important for further development.

AgNPs have been reported as antimicrobials which attack to the cell membrane containing sulfur-containing proteins and penetrate inside the bacterial cell. Then the AgNPs interact with proteins in the cell as well as with the phosphorus-containing compounds like DNA. They preferably attack the respiratory chain and cell division, finally leading to cell death (Rai, 2009). Moreover, the AgNPs can induce enhanced level of reactive species (ROS) production in the intracellular compartment of bacterial cells, causing disruption of biomolecule within cells (Xu, 2012)

In 2010, Li et al analyzed the growth, permeability, and the direct observation of morphological change of the bacterial cells after treatment with AgNPs by transmission electron microscope (TEM) and scanning electron microscope (SEM). TEM and SEM observation which can be visually noticed the morphological change and some surface changes, but no roughness of surface change and height change in detail was shown. Therefore, we will investigate imaging techniques for surface analysis and height of bacteria (Li, 2010).

Atomic force microscopy (AFM) is a technique which can be used to analyze the surface morphology of bacterial cells, as it combines greatly improved resolution compared with optical microscopy (La Storia, 2011) and has potential as an effective tool to understand mode of action of antimicrobial peptide, antibiotic and antimicrobial agent (Li, 2007). For example, da Silva and Teschke studied antimicrobial effect of antimicrobial peptide PGLa on *E. coli* both in physiological medium and in air (Da Teschke, 2003) Formosa et al studied nanoscale effects of antibiotics (tobramycin and ticarcillin) on *Pseudomonas aeruginosa* (Formosa et al., 2012) and Yang et al investigated the characteristic effects of silver ion on *E. coli* and *Staphylococcus epidermidis* (Yang et al., 2010). The AFM can be acquired images of morphology, surface roughness, and three-dimensional images including height of bacterial cell (Alves, 2010).

However, the kinetics evidence of the AgNPs killing mechanism on bacterial cells is no clear. In this study, we focused on the antimicrobial mechanism of AgNPs against the *E. coli* O157:H7 cell and used AFM to investigate morphological change of bacterial cells.

Objectives of the study

We determined the mechanism of action of AgNPs on *E. coli* O157:H7 cells and investigated the antimicrobial mechanism of AgNPs on the *E. coli* O157:H7 cell using AFM.

Methodology

Bacterial strains and growth conditions

E. coli O157:H7 stored at -70°C in 20% glycerol were streaked in the agar medium. They were incubated at 37°C overnight. The colonies were picked up and cultured in Mueller Hinton Broth (MHB) and shaking at 37°C overnight in160 rpm shaker-incubator. The overnight culture was then subcultured for 2-3 hours for a mid-logarithmic growth phase culture (Madhongsa et al., 2013).

Determination of minimum inhibitory concentration (MIC) and minimum bactericidal concentration (MBC)

MIC of AgNPs against *E. coli* O157:H7 was determined by broth microdilution method (Lv et al., 2014). Briefly, the bacterial suspensions were prepared and added to range of concentrations (0.125, 0.25, 0.5, 1, 2, 4, 8, 16, 32 and 64 µg/ml) of AgNPs was prepared by serial dilution in each well of 96-well plate. The plate was incubated at 37°C for 20 hours. The MIC was defined as the lowest concentration of AgNPs that completely inhibited the bacterial growth (Shin et al., 2013). Each MIC test was carried out in 2 independent experiment triplicates. The 10 µl of no turbidity in the well was dropped on MHA and further incubated at 37°C overnight. The MBC value was corresponded to the lowest concentration that could inhibit 99.9% of bacterial growth (Mataraci et al., 2012)

Time-kill assay of antimicrobial activity

The time-kill kinetics change was determined on the bacterial growth curve. The single colony of *E. coli* O157:H7 was cultured in MHB at 37°C and then subcultured until reached a mid-logarithmic phase of bacterial growth. Then 250 µl of adjusted inoculum with final concentration of $1X10^7$ CFU/ml was added to microtube containing 250 µl AgNPs which was defined as MIC. The suspension was then incubated at 37°C with shaking at 160 rpm. At 0, 5, 10, 15, 30, 45, 60 min and 3, 5, 24 h, serial 10-fold dilutions were performed in deionize water and 10 µl of solution was dropped on MHA and further incubated at 37°C, overnight. Colony count method was assayed. Bactericidal activity was defined as a reduction of 99.9% or □ 3 $\log_{10}$ of the total count of CFU per milliliter in the original bacteria (Pankey & Ashcraft, 2009).

ROS production assay

ROS are signaling pathway of cell death. ROS of *E. coli* O157:H7 cells induced by AgNPs were determined using an oxidation-sensitive probe 2□, 7□-dichlorofluorescin diacetate (DCFH-DA) (Tian et al., 2006). DCFH-DA positively diffuses through the cell membrane into the cell and is deacetylated by esterase to form non-fluorescence 2□, 7□-dichlorohydrofluorescin (DCFH). DCFH reacts with ROS to form the fluorescence 2□, 7□-dichlorofluorescin (DCF) trapped inside the cell, marking the cell fluorescence. For the experiment, bacterial colonies were picked and cultured in MHB at 37°C, overnight with shaking at 160 rpm. Then the inoculum was subcultured and incubated at 37°C in a 160 rpm shaker-incubator for 2-3 h to reach a mid-logarithmic growth phase culture. The cell suspension was centrifuged at 10,000 g for 5 min and diluted to $1X10^7$ CFU/ml. After that, the cells were washed twice time with 10 mM potassium phosphate buffer (PPB) to remove the probe outside the cell and re-suspended in the same buffer. DCFH-DA was mixed with the cell suspension at a ratio of 1:20 and the mixture was shaken for 60

min at 37°C in the dark to successfully load the fluorescence probe into the cell. The cell suspension was centrifuged and washed twice with 10 mM PPB to remove the probe outside the cells. Add the final concentration of AgNPs at MIC and incubated for 0, 5, 10, 15, 30, 45, 60 min and 2, 3, 5 h to investigate kinetics and quantitate the generation of ROS. The fluorescence intensity of DCF was detected by fluorescence spectrophotometer (SpectraMax M5) at excitation and emission wavelength of 488 and 535 nm, respectively (Xu et al., 2012).

AFM imaging

The AFM images were taken in air with a Park system. Measurements of non-contact mode and contact mode were silicon nitride cantilever (PPP-NCHR) using with resonance frequencies of approximately 330 kHz and force constants of approximately 42 Nm^{-1}. Height and topography images were scanned at 1-0.7 Hz.

Preparation of bacterial samples

Colonies were picked and cultured in MHB and the bacterial culture was grown overnight at 37°C in a 160 rpm shaker-incubator. The inoculum was then subcultured until reached a mid-logarithmic phase of bacteria growth. The bacterial cells were harvested and washed in phosphate buffer saline (PBS). A 10 ml of bacterial suspension ($1x10^7$ CFU/ml) was combined with 300 µl of 100 mM *N*-(3-Dimethylaminopropyl)-*N*□-ethylcarbodiimide hydrochloride (pH 5.5, EDC, Sigma-Aldrich) and 300 µl of 40 mM *N*-hydroxysulfosuccinimide (pH 7.5, Sulfo-NHS, Sigma-Aldrich for 10 min. (Strauss et al., 2009).

Glass slide was rinsed with ultrapure water and methanol, immersed in 30% 3-aminopropyltriethoxysilane in methanol (Sigma-Aldrich) for 20 min. and then rinsed with ultrapure water. Bacterial solution was added to the glass slide for 1-2 hours to promote bacterial lawn formation before imaging was carried out.

Results

MIC of AgNPs

Antimicrobial activity of AgNPs against *E. coli* O157:H7 was assessed by measurement of its MIC and MBC (Table 1). The AgNPs were identified to be potentially active against *E. coli* O157:H7 with MIC and MBC of 16 µg/ml.

Table 1 The MIC and MBC of AgNPs against *E. coli* O157:H7

Optical density ($OD_{600\ nm}$)	**MIC (µg/ml)**		**MBC (µg/ml)**	
	AgNPs	Polymyxin B	AgNPs	Polymyxin B
0.01 ($1X10^7$ CFU/ml)	16	2	16	2

Kinetics of bactericidal activity and percentage of bacterial growth inhibition

In the time–kill assay, kinetics of the antibacterial activity of the AgNPs at MIC value against *E. coli* O157:H7 was detected. The AgNPs showed rapid action, resulting in 88**%** bacterial killing within 5 min. Then, bacterial growth was inhibited at 99.9% or bactericidal activity of the AgNPs was defined as >3 $\log_{10}$ CFU/mL within 1 h (Fig. 1).

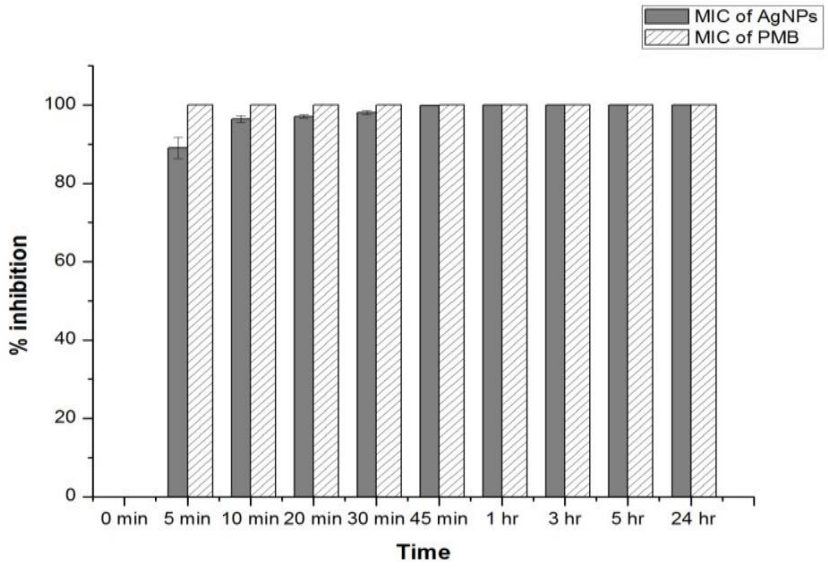

Figure 1 The percentage of bacterial growth inhibition of AgNPs against *E.coli* O157:H7 that polymyxin B (PMB) as positive control. The value was calculated from time-kill assay.

ROS production assay

We used the DCFH-DA dye, which can produce green fluorescence in the presence of ROS. This dye is able to penetrate the membranes of living cells and it can detect ROS in both living cells and dead cells. AgNPs are known to induce the accumulation of ROS in side bacterial cells. The *E. coli* O157:H7 cells after exposure to MIC of AgNPs was measured. The ROS of *E. coli* O157:H7 cells were slowly produced within the 1 h after exposure to the AgNPs. After that, ROS production showed increasingly at 2-5 hours when compared with untreated cells (Fig. 2).

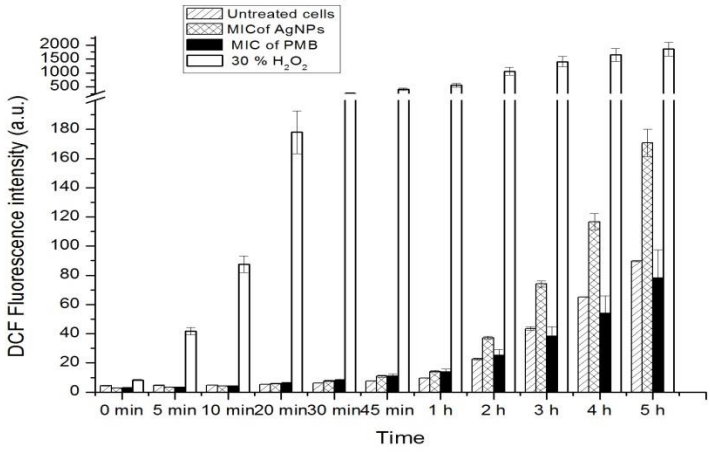

Figure 2 The kinetics of ROS production in *E. coli* O157: H7 after exposure to AgNPs. Quantitative ROS determination in bacterial cells by DCF fluorescence intensity. The untreated cells as negative control and 30% H_20_2 as positive control.

Effect of AgNPs on *E. coli* O157:H7 analysis using AFM imaging

Morphological changes of *E. coli* after treated with AgNPs

The AFM imaging of *E. coli* untreated cells displayed rod shape structure and smooth surface without rupture and damage (Fig. 3A and 3E). When *E. coli* cell was treated with 1/4 MIC of AgNPs, representing cells retained rod-like form. However, bacterial cell showed minor lesion at the head region of cells (Fig. 3B and 3F). At 1/2 MIC of AgNPs, bacterial cells showed morphological change of membrane surface and vesicles appeared (Fig. 3C and 3G). At MIC of AgNPs, the bacterial cells were ruptured and cytoplasmic content was leaked (Fig. 3D and 3H). The results indicated that the effect of bacterial killing was depended on concentration of AgNPs.

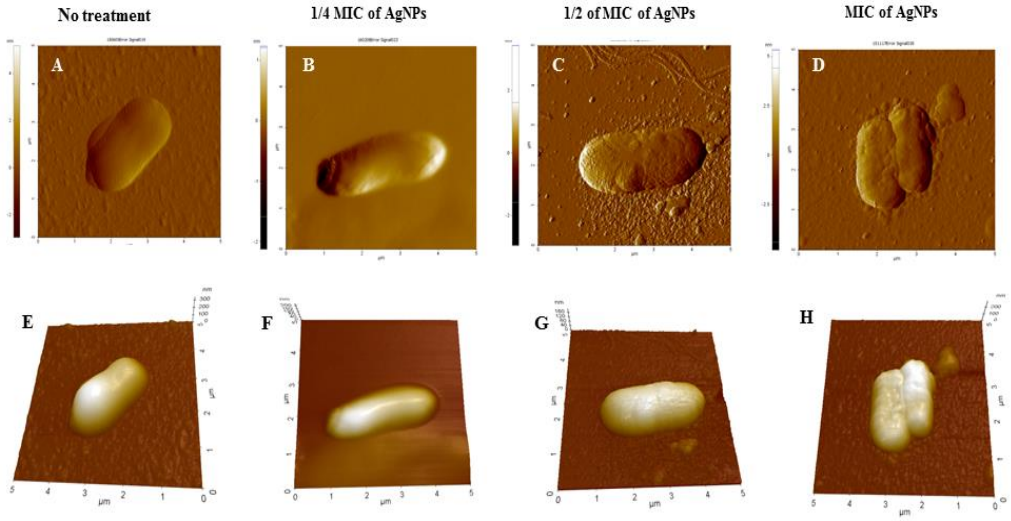

Figure 3 Dose dependent of AgNPs effects on *E. coli* imaged by AFM. A-D are error signal images and E-H are three-dimensional images of *E. coli* cells. A and E, untreated cells, B and F, *E. coli* cell which was treated with 1/4 MIC, C and G, *E. coli* cells treated with 1/2 MIC, D and H, and treated *E. coli* cells with MIC

Height change of *E. coli* O157:H7 cells

To monitor the height change of AgNPs treatment on the *E. coli* O157:H7, AFM images of a typically untreated *E. coli* bacterium dried in air are presented in Fig. 4. Fig. 4A shows topography image and 4B shows three-dimensional image. The native *E. coli* cell shows rod shaped morphology. The *E. coli* cell are approximately 2 µm large (green line Fig. 4D), approximately 3 µm long (red line Fig.4D) and approximately 250 nm high (green line Fig. 4D). While *E. coli* cell was then treated with the MIC of AgNPs for 1 hour as presented in Fig. 5. The AFM images of *E. coli* cell change in size are approximately 1.5 µm large (green line Fig. 5D), approximately 2 µm long (red line Fig. 5D) and approximately 160 nm high (green line Fig. 5D). The results indicated that the height of bacterial cell was decreased when treated with MIC of AgNPs.

In addition, measurement of average height of *E. coli* O157:H7 when treated with the MIC of AgNPs, it displayed approximately 164.5±46.0 nm (n=8) which was decreased when compared with *E. coli* O157:H7 untreated cells that showed approximately 237.6± 16.7 nm (n= 8) (Table 2). Therefore, the AgNPs have damage to *E. coli* O157:H7 cells.

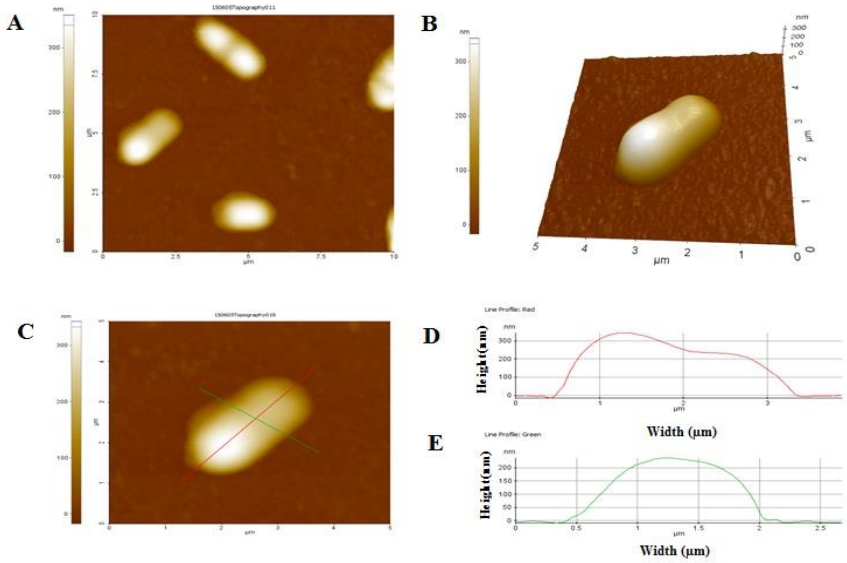

Figure 4 Atomic force microscopy images of untreated *E. coli* O157:H7 cell which was dried in air. A and C, topographic images were scanned area for images 10x10 µm^2 (A) and 5x5 µm^2 (C). B, three-dimensional images. D, vertical cross-section was taken along the red line. E, horizontal cross-section was taken along the green line.

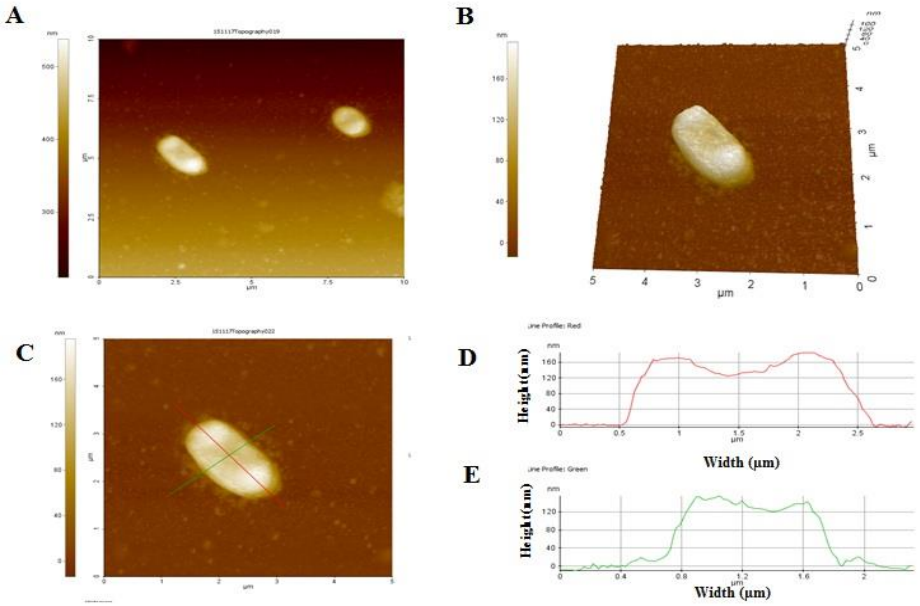

Figure 5 AFM image of treated *E. coli* O157:H7 with AgNPs at MIC value within 1 hour. A and C, topographic images were scanned area for images 10x10 µm^2 (A) and 5x5 µm^2 (C). B, three-dimensional images. D, vertical cross-section was taken along the red line. E, horizontal cross-section was taken along the green line.

Surface roughness analysis of *E.coli* O157:H7 cells

To evaluate the damage of *E. coli* O157:H7 that was exerted by MIC value of AgNPs, AgNPs completely disrupted the bacterial cells. Thus surface roughness measurements were compared between the treated bacterial cells with AgNPs at MIC value and untreated cells that as control. The untreated cells had less surface roughness than treated bacterial cells with AgNPs at MIC value (Fig. 6). In addition, treated *E. coli* O157:H7 with MIC value of AgNPs was calculated as the root mean square roughness (Rq), it displayed approximately 17.6±3.5 nm (n=8) while untreated *E. coli* O157:H7 cell showed approximately 11.5±1.5 nm (n=8) (Table 2). Therefore, AgNPs can disrupt and damage the surface of *E. coli* O157:H7 membrane.

Table 2 Measurement of AFM parameters from *E. coli* O157:H7.

***E. coli* O157:H7**	**Bacterium average height H (nm)**	**Rq (nm)**
Untreated	237.6± 16.7	11.5±1.5
AgNPs (10-20 nm)	164.5±46.0	17.6±3.5

The height represents the maximum cell height and Rq represents the root mean square roughness.

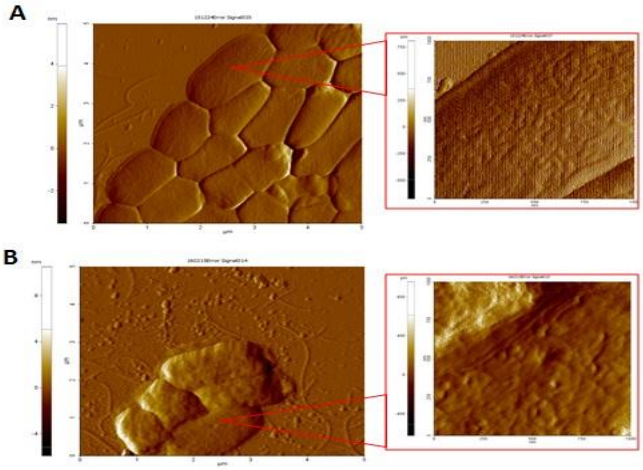

Figure 6 AFM image shows surface roughness of *E. coli* O157:H7. A; untreated cell and B; treated cell with AgNPs as MIC within 1 hour.

Discussion and Conclusion

In this study, we measured the MIC of AgNPs against *E. coli* O157:H7. The results showed that AgNPs have potential effect against *E .coli* O157:H7 at 16 µg/ml and completely showed bactericidal activity within 1 hour. While, the bacterial cells produced ROS after exposure AgNPs within 2-5 hours. In under normal condition, the bacterial cells produced non-toxic of ROS from intracellular metabolites. When bacterial cells were induced by stress, they produce a lot of ROS in the cells that these ROS are caused of bacterial cell death (Zhao et al., 2010). In the results, we found that AgNPs can kill *E. coli* O157:H7 before cells produced a lot of ROS. Therefore, ROS produced is not related with cells death. The AFM imaging showed 1/4 MIC of AgNPs still not make a change on *E. coli* cell, remained smooth surface of *E. coli* cell was determined. When the concentration of AgNPs was increased to 1/2 of MIC, bacterial vesicle was then appeared on surface membrane. After treated bacterial cells at MIC value of AgNPs, bacterial cells was completely shown in membrane damage. This is AgNPs concentration-dependent. AFM image showed the effect of treated *E. coli* with AgNPs at MIC concentration within 1 hour and the results showed that *E. coli* was damaged on the membrane, changed in morphology, shown roughness surface, collapsed and leakage of cytosol .In addition, untreated bacteria cells was decreased their height from 237.6±16.7 nm to 164.5±46.0 nm when the cell was treated with AgNPs at MIC value. The surface of the untreated bacterial cells showed less roughness (11.5±1.5 nm) than treated bacterial cells with MIC of AgNPs (17.6±3.5nm). The *E. coli* belongs to the Gram-negative bacteria, which consisting outer membrane and a thin peptidoglycan layer. The outer membrane consists of lipopolysaccharide (LPS), which have negatively charged of phosphate group (da & Teschke, 2003). AgNPs will released silver ion (Ag^{+}) that can interact with negatively charged on bacterial cells (Kalishwaralal et al., 2010) with electrostatic force. When the Ag^{+} attack cell membrane, they accumulated in bacterial membrane resulted in the membrane exhibited “pits ”and the increase in permeability leading to the death of bacterial cells (Sondi et al., 2004). However, if concentration of Ag^{+} less than MIC, the bacterial cells had self-defensed by produce vesicle on cellular

surface. Thefore, we proposed mechanism of action of AgNPs that involve in 2 phases: initial, AgNPs show the bacterial killing by membrane damage mechanism and after that increase in ROS production.

Acknowledgements

The student scholarship is supported by Protein and Proteomics Research Center for Commercial and Industrial Purposes, Khon Kaen University. The instrument service (Atomic force microscopy) was provided by Research Instrument Center, Khon Kaen University, Thailand.

References

Alves CS, Melo MN, Franquelim HG, Ferre R, Planas M, Feliu L, et al. *Escherichia coli* cell surface perturbation and disruption induced by antimicrobial peptides BP100 and pepR. The Journal of Biological Chemistry. 2010;285(36):27536-44.

Appelbaum PC. Antimicrobial resistance *in Streptococcus pneumoniae*: an overview. Clinical Infectious Diseases.1992;15(1):77-83.

Da Silva A, Jr., Teschke O. Effects of the antimicrobial peptide PGLa on live *Escherichia coli*. Biochimica et Biophysica Acta. 2003;1643(1-3):95-103.

Formosa C, Grare M, Duval RE, Dague E. Nanoscale effects of antibiotics on *P. aeruginosa*. Nanomedicine: Nanotechnology, Biology and Medicine. 2012;8(1):12-6.

Kalishwaralal K, BarathManiKanth S, Pandian SRK, Deepak V, Gurunathan S. Silver nanoparticles impede the biofilm formation by *Pseudomonas aeruginosa* and *Staphylococcus epidermidis*. Colloids and Surfaces B: Biointerfaces. 2010;79(2):340-4

La Storia A, Ercolini D, Marinello F, Di Pasqua R, Villani F, Mauriello G. Atomic force microscopy analysis shows surface structure changes in carvacrol-treated bacterial cells. Research in Microbiology. 2011;162(2):164-72.

Li A, Lee PY, Ho B, Ding JL, Lim CT. Atomic force microscopy study of the antimicrobial action of Sushi peptides on Gram negative bacteria. Biochimica et Biophysica Acta. 2007;1768(3):411-8.

Li WR, Xie XB, Shi QS, Zeng HY, Ou-Yang YS, Chen YB. Antibacterial activity and mechanism of silver nanoparticles on *Escherichia coli*. Applied Microbiololy and Biotechnology. 2010;85(4):1115-22.

Lv Y, Wang J, Gao H, Wang Z, Dong N, Ma Q, et al. Antimicrobial properties and membrane-active mechanism of a potential α-helical antimicrobial derived from cathelicidin PMAP-36. PLoS One. 2014;9(1):e86364.

Madhongsa K, Pasan S, Phophetleb O, Nasompag S, Thammasirirak S, Daduang S, et al. Antimicrobial action of the cyclic peptide bactenecin on Burkholderia pseudomallei correlates with efficient membrane permeabilization. PLoS neglected tropical diseases. 2013;7(6):e2267.

Mataraci E, Dosler S. In Vitro Activities of antibiotics and antimicrobial cationic peptides alone and in combination against methicillin-resistant *staphylococcus aureus* biofilms. Antimicrobial Agents and Chemotherapy. 2012;56(12):6366-71.

Pankey GA, Ashcraft DS. In vitro antibacterial activity of tigecycline against resistant Gram-negative bacilli and enterococci by time-kill assay. Diagnostic Microbiology and Infectious Disease. 2009;64(3):300-4.

Rai M, Yadav A, Gade A. Silver nanoparticles as a new generation of antimicrobials. Biotechnology Advances. 2009;27(1):76-83

Shin JR, Lim KJ, Kim DJ, Cho JH, Kim SC. Display of multimeric antimicrobial peptides on the *Escherichia coli* cell surface and its application as whole-cell antibiotics. PLoS One. 2013;8(3):e58997.

Sondi I, Salopek-Sondi B. Silver nanoparticles as antimicrobial agent: a case study on *E. coli* as a model for Gram-negative bacteria. Journal of Colloid and Interface Science. 2004;275(1):177-82.

Strauss J, Burnham NA, Camesano TA. Atomic force microscopy study of the role of LPS O-antigen on adhesion of E. coli. Journal of Molecular Recognition . 2009;22(5):347-55.

Tian Y-Y, An L-J, Jiang L, Duan Y-L, Chen J, Jiang B. Catalpol protects dopaminergic neurons from LPS-induced neurotoxicity in mesencephalic neuron-glia cultures. Life Sciences. 2006;80(3):193-9.

Xu H, Qu F, Xu H, Lai W, Andrew Wang Y, Aguilar ZP, et al. Role of reactive oxygen species in the antibacterial mechanism of silver nanoparticles on *Escherichia coli* O157:H7. Biometals. 2012;25(1):45-53.

Yang X, Yang W, Wang Q, Li H, Wang K, Yang L, et al. Atomic force microscopy investigation of the characteristic effects of silver ions on *Escherichia coli* and *Staphylococcus epidermidis*. Talanta. 2010;81(4–5):1508-12.

Zhao X, Drlica K. Reactive oxygen species and the bacterial response to lethal stress. Current Opinion in Microbiology. 2014;0:1-6.